Hindawi
Advances in Mathematical Physics
Volume 2023, Article ID 9974539, 10 pages
https://doi.org/10.1155/2023/9974539

*Research Article*

# High-Order Spectral Method of Density Estimation for Stochastic Differential Equation Driven by Multivariate Gaussian Random Variables

**Hongling Xie** [1,2]

[1]*School of Statistics and Mathematics, Yunnan University of Finance and Economics, Kunming 650221, Yunnan, China*
[2]*School of Mathematics and Statistics, Honghe University, Mengzi 661100, Yunnan, China*

Correspondence should be addressed to Hongling Xie; xiehongling316@163.com

Received 5 August 2022; Revised 11 March 2023; Accepted 28 March 2023; Published 16 August 2023

Academic Editor: Sayyouri Mhamed



There are some previous works on designing efficient and high-order numerical methods of density estimation for stochastic partial differential equation (SPDE) driven by multivariate Gaussian random variables. They mostly focus on proposing numerical methods of density estimation for SPDE with independent random variables and rarely research density estimation for SPDE is driven by multivariate Gaussian random variables. In this paper, we propose a high-order algorithm of gPC-based density estimation where SPDE driven by multivariate Gaussian random variables. Our main techniques are (1) we build a new multivariate orthogonal basis by adopting the Gauss–Schmidt orthogonalization; (2) with the newly constructed orthogonal basis in hand, we first assume the unknown function in the SPDE has the stochastic general polynomial chaos (gPC) expansion, second implement the stochastic gPC expansion for the SPDE in the multivariate Gaussian measure space, and third we obtain and numerical calculation deterministic differential equations for the coefficients of the expansion; (3) we used high-order algorithm of gPC-based for density estimation and moment estimation. We apply the newly proposed numerical method to a known random function, stochastic 1D wave equation, and stochastic 2D Schnakenberg model, respectively. All the presented stochastic equations are driven by bivariate Gaussian random variables. The efficiency is compared with the Monte-Carlo method based on the known random function.

## 1. Introduction

In modern science, no matter numerical model or physical model, the study of uncertainty (randomness) is more important and concerned. Such uncertainties arise from one or more parameters of the model, sometimes related to each other. Because of such uncertain parameters, the solution of the model is also uncertain. For example, in the field of biochemistry [1–3], in the field of structural engineering [3, 4], and in hydrology engineering [3, 5].

For the random solution, there are usually two main research aspects of moment estimation and density estimation from the perspective of statistical properties. The research of moment estimation, such as mean (expectation) and variance, is based on obtaining the numerical solution of the model by numerical calculation. The most direct method to obtain numerical solutions is the Monte-Carlo method, which takes samples from the sample space of parameters describing randomness, assigns values to random parameters, and numerically calculates the random solutions. However, this method has a large amount of calculation and a low convergence rate [6]. If high precision approximation is required, stochastic general polynomial chaos (gPC) expansion is a preferred choice, such as the stochastic Galerkin spectral method. We also can consider the stochastic perturbation-based finite element method, and this method is a very efficient alternative for higher-order spectral methods. The theoretical basis of the method is Taylor's expansion of all uncertain parameters and state functions [7].

For the stochastic Galerkin spectral method, how to use the weight function of random variables (joint probability density function) to find the orthogonal basis is a major

challenge. Especially when dealing with multivariate random variables, a multivariate orthogonal basis is difficult to find [8].

Orthogonal basis can be used in relevant methods, including measure-consistent chaos expansion [9, 10], domination method [11], Gauss–Schmidt orthogonalization [12–18], and mapping transformation method [8, 11, 19, 20]. After obtaining the approximation of the random function, the moment estimation can be carried out, and the mean or variance of the random solution can be estimated as a whole.

In this paper, we discuss the differential equations driven by multivariate Gaussian random variables. On the basis of moment estimation, we estimate the density of random solution. When the random variable is univariate, standard kernel density estimation [3, 21, 22] can be used from a statistical point of view. In the study of Ditkowski et al. [3], numerical solutions of random functions and density of stochastic differential equations driven by univariate random variables and multivariate linear independent random variables are discussed, mainly gPC-based estimation and Spline-based estimation. For the multivariate random variable (DEPENDENT) situation, it introduced briefly the application of multivariate-spline-based estimation [3].

Based on the above excellent results and methods, this paper aims at differential equations driven by multivariate random Gaussian variables. A high-order algorithm of gPC-based for density estimation based on polynomial chaos expansion is designed to estimate the moment and density of the random solution [3]. Our main techniques are (1) we build a new multivariate orthogonal basis by adopting the Gauss–Schmidt orthogonalization; (2) with the newly constructed orthogonal basis in hand, we first assume the unknown function in the stochastic partial differential equation (SPDE) has the stochastic gPC expansion, second implement the stochastic gPC expansion for the SPDE in the multivariate Gaussian measure space, and third we obtain and numerical calculation deterministic differential equations for the coefficients of the expansion; (3) we used high-order algorithm of gPC-based for density estimation and moment estimation. We apply the newly proposed numerical method to a known random function, stochastic 1D wave equation, and stochastic 2D Schnakenberg model, respectively. The efficiency is compared with the Monte-Carlo method based on the known random function.

This article is organized as follows: in Section 2, we discuss the high-order stochastic chaos expansion of random functions and introduce the stochastic Galerkin spectral method and the high-order approximation of the expansion coefficients. In Section 3, the high-order algorithm of gPC-based for density estimation based on polynomial chaos expansion is introduced, and the numerical calculation process of moment estimation and density estimation is introduced. In Section 4, the moment and density estimation of a known random function are calculated numerically, and the efficiency problem is compared with the Monte-Carlo method. The proposed algorithm is applied to stochastic 1D wave equation and stochastic 2D Schnakenberg model. In Section 5, the algorithm and numerical results proposed in this paper are summarized.

## 2. High-Order Stochastic gPC Expansion

We consider the boundary value problem of SPDE driven by multivariate Gaussian measure

$$\begin{cases} \mathscr{L}u(\vec{x},\xi(\omega)) = h(\vec{x},f(\xi(\omega))),\ \vec{x}\in D\subset\mathbb{R}^d, \\ \mathscr{B}u(\vec{x},\xi(\omega)) = g(\vec{x},f(\xi(\omega))),\ x\in\partial D, \end{cases} \tag{1}$$

where the unknown function $u = u(\vec{x},\xi(\omega))$. $\vec{x}$ is the spatial variable, $\mathscr{L},\mathscr{B}$ are some differential operator with respect to $\vec{x}$. $\xi(\omega)\in\mathbb{R}^K$ is a $K$-dimensional random vector with Gaussian measure. $f,h,g$ are some known function. $\xi(\omega)$ is the $K$-dimensional vector of random input variables, whose Joint probability density function $\rho(\vec{y})$ $(\vec{y}\in\mathbb{R}^K)$. $\xi = (\xi_1,\xi_2,\ldots,\xi_K)$ typically represents the uncertainties in the model [8, 23].

*2.1. Stochastic General Polynomial Chaos Expansion.* Given a finite nonnegative integer $N$ and $K$, we define a truncated multi-indices set as follows [24]:

$$\mathscr{J}^{N,K} = \left\{\alpha = (\alpha_1,\ldots,\alpha_K)|\alpha_i\in\{0,\ldots,N\},|\alpha| = \sum_{i=1}^{K}\alpha_i\le N\right\}. \tag{2}$$

The polynomial chaos expansion for random input functions $f(\xi)$, $h(\vec{x},\xi)$, and $g(\vec{x},\xi)$ and the unknown function $u(\vec{x},\xi)$ [8]

$$\begin{aligned} f^{N,K}(\xi) &= \sum_{\alpha\in\mathscr{J}^{N,K}}\widehat{f}_\alpha\Phi_\alpha(\xi), \\ h^{N,K}(\vec{x},\xi) &= \sum_{\alpha\in\mathscr{J}^{N,K}}\widehat{h}_\alpha(\vec{x})\Phi_\alpha(\xi), \\ g^{N,K}(\vec{x},\xi) &= \sum_{\alpha\in\mathscr{J}^{N,K}}\widehat{g}_\alpha(\vec{x})\Phi_\alpha(\xi), \\ u^{N,K}(\vec{x},\xi) &= \sum_{\alpha\in\mathscr{J}^{N,K}}\widehat{u}_\alpha(\vec{x})\Phi_\alpha(\xi), \end{aligned} \tag{3}$$

where the polynomial chaos orthogonal basis $\{\Phi_\alpha(\xi),\alpha\in\mathscr{J}^{N,K}\}$ can be constructed with Gauss–Schmidt orthogonalization method (more details, see [18]). Then, we can obtain the following finite-dimensional and deterministic PDE problem: for all $\Phi_\beta$, finding $u^{N,K}$ such that

$$\begin{aligned} \mathbb{E}\left[\mathscr{L}u^{N,K}(\vec{x},\xi)\Phi_\beta(\xi)\right] &= \mathbb{E}\left[h^{N,K}(\vec{x},\xi)\Phi_\beta(\xi)\right],\ \vec{x}\in D\subset\mathbb{R}^d, \\ \mathbb{E}\left[\mathscr{B}u^{N,K}(\vec{x},\xi)\Phi_\beta(\xi)\right] &= \mathbb{E}\left[g^{N,K}(\vec{x},\xi)\Phi_\beta(\xi)\right],\ \vec{x}\in\partial D. \end{aligned} \tag{4}$$

*2.2. Higher-Order Calculation of Coefficients.* In order to high-order to solve Equation (4), the calculation of coefficients $\widehat{u}_\alpha(\vec{x})$ as follows:

$$\begin{aligned}\widehat{u}_\alpha(\vec{x}) &= \mathbb{E}[u^{N,K}(\vec{x},\xi_1,\ldots,\xi_K)\Phi_\alpha(\xi_1,\ldots,\xi_K)]\\ &= \int_{-\infty}^{\infty}\cdots\int_{-\infty}^{\infty}u^{N,K}\Phi_\alpha(\xi_1,\ldots,\xi_K)\rho(\xi_1,\ldots,\xi_K)d\xi_K\ldots d\xi_1.\end{aligned} \tag{5}$$

Denote the integral transformation for $\xi=(\xi_1,\ldots,\xi_K)$

$$\xi_i=\frac{\eta_i}{1-\eta_i^2},\ i=1,2,\ldots,K, \tag{6}$$

where $\eta=(\eta_1,\eta_2,\ldots,\eta_K)$. Then Equation (5) can be rewritten as follows:

$$\begin{aligned}u_\alpha(\vec{x}) &= \int_{-\infty}^{\infty}\cdots\int_{-\infty}^{\infty}u^{N,K}\Phi_\alpha(\xi_1,\ldots,\xi_K)\rho(\xi_1,\ldots,\xi_K)d\xi_K\ldots d\xi_1\\ &= \int_{-1}^{1}\cdots\int_{-1}^{1}u^{N,K}\Phi_\alpha(\eta)\rho(\eta)\frac{1+\eta_K^2}{(1-\eta_K^2)^2}\cdots\frac{1+\eta_1^2}{(1-\eta_1^2)^2}d\eta_K\ldots d\eta_1.\end{aligned} \tag{7}$$

We choose mesh sizes $\Delta\eta_i>0$, $(i=1,2,\ldots,K)$ with $\Delta\eta_i=2/S_i$ for $S_i$ even positive integers, and let the grid points be as follows:

$$\eta_{i,j}=-1+j\Delta\eta_i,\ j=1,2,\ldots,S_i-1. \tag{8}$$

Then Equation (7) can be rewritten as follows where used trapezoidal rules, denotes

$$\mathcal{J}(\eta_1,\ldots,\eta_K)=u^{N,K}(\vec{x},\eta_1,\ldots,\eta_K)\Phi_\alpha(\eta_1,\ldots,\eta_K)\rho(\eta_1,\ldots,\eta_K)\frac{1+\eta_K^2}{(1-\eta_K^2)^2}\cdots\frac{1+\eta_1^2}{(1-\eta_1^2)^2}, \tag{9}$$

$$\begin{aligned}\mathbb{I} &= \sum_{j_1=1}^{S_1-1}\cdots\sum_{j_K=1}^{S_K-1}\int_{\eta_1,j_1}^{\eta_{1,j_1+1}}\cdots\int_{\eta_{K,j_K}}^{\eta_{K,j_K+1}}\mathcal{J}(\eta_1,\ldots,\eta_K)d\eta_K\ldots d\eta_1\\ &= \sum_{j_1=1}^{S_1-1}\cdots\sum_{j_K=1}^{S_K-1}\mathcal{J}\left(\eta_{1,j_1},\eta_{2,j_2}\ldots,\eta_{K-1,j_{K-1}},\eta_{K,j_K}\right)\\ &\quad+\mathcal{J}\left(\eta_{1,j_1},\eta_{2,j_2}\ldots,\eta_{K-1,j_{K-1}},\eta_{K,j_K+1}\right)\\ &\quad+\mathcal{J}\left(\eta_{1,j_1},\eta_{2,j_2}\ldots,\eta_{K-1,j_{K-1}+1},\eta_{K,j_K}\right)\\ &\quad+\mathcal{J}\left(\eta_{1,j_1},\eta_{2,j_2}\ldots,\eta_{K-1,j_{K-1}+1},\eta_{K,j_K+1}\right)\\ &\quad+\ldots\ \ldots\ \ldots\ \ldots\ \ldots\ \ldots\ \ldots\\ &\quad+\mathcal{J}\left(\eta_{1,j_1},\eta_{2,j_2+1}\ldots,\eta_{K-1,j_{K-1}+1},\eta_{K,j_K}\right)\\ &\quad+\mathcal{J}\left(\eta_{1,j_1},\eta_{2,j_2+1}\ldots,\eta_{K-1,j_{K-1}+1},\eta_{K,j_K+1}\right)\\ &\quad+\mathcal{J}\left(\eta_{1,j_1+1},\eta_{2,j_2+1}\ldots,\eta_{K-1,j_{K-1}+1},\eta_{K,j_K}\right)\\ &\quad+\mathcal{J}\left(\eta_{1,j_1+1},\eta_{2,j_2+1}\ldots,\eta_{K-1,j_{K-1}+1},\eta_{K,j_K+1}\right),\end{aligned} \tag{10}$$

$$\widehat{u}_\alpha(\vec{x})=\frac{\mathbb{I}}{2^K}\prod_{i=1}^{K}\Delta\eta_i=\frac{\mathbb{I}}{2^K}\prod_{i=1}^{K}\frac{2}{S_i}=\frac{\mathbb{I}}{\prod_{i=1}^{K}S_i}. \tag{11}$$

In order to high-order approximation, the length of every dimension $S_i$ needs to a lot more than usual.

## 3. Density and Moment Estimation

For random function $u=u(\vec{x},\xi(\omega))$, we may wish to know its statistical properties as follows:

1. Moment estimation.

$$\mathbb{E}[u]=\int_D u(\xi(\omega))\rho(\xi(\omega))d\xi(\omega),\ Var[u]=\mathbb{E}[u^2]-[\mathbb{E}[u]]^2. \tag{12}$$

2. Density estimation.

$$p(z)=\frac{dP(z)}{d(z)}, \tag{13}$$

where $P$ is the cumulative distribution of $u$, $\vec{z}\in\mathbb{R}^K$.

*3.1. Higher-Order Algorithm of gPC-Based*

*3.2. Accuracy of Algorithm.* The error of density estimation comes from the approximation for $u(\vec{x},t,\xi)$. Denote $M=(K+N)/!K!N!-1$ and the set $\{\Phi_\alpha(\xi),\ \alpha\in\mathcal{J}^{N,K}\}$ equal to $\{\Phi_m(\xi),m=0,1,\ldots,M\}$.

$$\left\|u(\xi)-\sum_{m=0}^{M}\widehat{u}_m\Phi_m(\xi)\right\|_2\sim Ce^{-\gamma M}. \tag{14}$$

For some constant $C,\gamma>0$ [3, 25–27].

$$|\mathbb{E}[u]-\mathbb{E}[u^{N,K}]|\le\|u-u^{N,K}\|_2, \tag{15}$$

$$|\mathrm{Var}(u)-\mathrm{Var}(u^{N,K})|\le(\sigma(u)+\sigma(u^{N,K}))\cdot\|u-u^{N,K}\|_2, \tag{16}$$

$$|\sigma(u)-\sigma(u^{N,K})|\le\|u-u^{N,K}\|_2, \tag{17}$$

where $\sigma(\cdot)$ represent standard deviation. If $u$ is analytic, the truncated expansion (Equation (3)) has the exponential accuracy [3, 27, 28].

## 4. Numerical Experiments

In this section, first, we text the accuracy of Algorithm 1 in moment estimation and density estimation for a known random function driven by bivariate Gaussian random variables.

(i) As integral transformation (Equation (6)).
(ii) For $i = 1, 2, \ldots, K$ and $j = 1, 2, \ldots, S_i - 1$, solve (Equation (4)) with $\eta = \eta_{i,j}$ to obtain $u(\vec{x}, \eta_{i,j})$.
(iii) Calculated $\widehat{u}_\alpha(\vec{x})$ based on Equation (10).
(iv) Approximate $u(\vec{x}, \xi) \approx u^{N,K}(\vec{x}, \xi) = \sum_{\alpha \in \mathcal{J}} \widehat{u}_\alpha(\vec{x}) \Phi_\alpha(\xi)$.
(v) Approximate $u(\tilde{\xi}) \approx u^{N,K}(\cdot, \tilde{\xi})$ on a sample of $\mathcal{S}_i \gg S_i$ points $\{\tilde{\xi}_i\}_{i,l=1}^{\mathcal{S}_i}$ which are according to $\rho(\xi)$.

(vi) Histogram method calculated PDF for $u$: $p_{\text{hist}}(z) := 1/\mathcal{S} \sum_{\ell=1}^{L} (\#\text{ of samples for which } u_l \in B_\ell) \cdot \mathbb{1}_{B_\ell}(z)$, $\mathbb{1}_{B_\ell}$ is the characteristic function of bin $B_\ell$ [3, 22].

If moment estimation is needed for $u$: $\mathbb{E}[u(\vec{x}, t, \xi)] \approx \mathbb{E}[u^{N,K}(\vec{x}, t, \xi)] = \widehat{u}_{\mathbf{0}}(\vec{x}, t)$,
$\text{Var}[u(\vec{x}, t, \xi)] \approx \text{Var}[u^{N,K}(\vec{x}, t, \xi)] = \sum_{\alpha \in \mathcal{J}} \widehat{u}_\alpha^2(\vec{x}, t)$,

where $\mathbf{0} \in \mathcal{J}, \mathbf{0} = (0, 0, \ldots, 0_K)$.

If density estimation needed for $G(u)$:
(vii) $G(u(\tilde{\xi})) \approx G(u^{N,K}(\cdot, \tilde{\xi}))$.
(viii) histogram method calculated $p_{\text{hist}}(z)$ for $G(u)$, the same as $u$.

Algorithm 1: gPC-based density estimation for multivariate Gaussian variables [3].

Secondly, let's apply Algorithm 1 for the stochastic 1D wave equation and stochastic 2D Schnakenberg model with the same random variables as the known random function.

The bivariate Gaussian random variables $(\xi_1, \xi_2) \sim N(\mu_1, \mu_2, \sigma_1^2, \sigma_2^2, R)$ (i.e., they are bivariate Gaussian random variables). $\mu_1, \mu_2, \sigma_1^2, \sigma_2^2, R$ are some known constants ($\mu_1 = \mu_2 = 1, \sigma_1^2 = \sigma_2^2 = 1, R = 0.6$ is taken in our calculation later).

The covariance of $(\xi_1, \xi_2)$ is $\begin{pmatrix} \sigma_1^2 & R\sigma_1\sigma_2 \\ R\sigma_1\sigma_2 & \sigma_2^2 \end{pmatrix}$.

The joint probability density of the bivariate Gaussian distribution is as follows:

$$\rho_\xi(y_1, y_2) = \frac{1}{2\pi\sigma_1\sigma_2\sqrt{1-R^2}} e^{\left[-\frac{(y_1-\mu_1/\sigma_1)^2 - 2R(y_1-\mu_1/\sigma_1)(y_2-\mu_2/\sigma_2) + (y_2-\mu_2/\sigma_2)^2}{2(1-R^2)}\right]}. \tag{18}$$

### 4.1. Example

*4.1.1. gPC Chaos.* We approximate a known random function with the truncated polynomial chaos expansion. Let the random function be defined as follows:

$$f(\xi_1, \xi_2) = \xi_1^2 - \xi_1\xi_2. \tag{19}$$

Let $N = 2, K = 2$, then $M = 5$. We numerically computed multivariate orthogonal polynomial basis based on Gauss–Schmidt orthogonalization method [18], the $\{\Phi_\alpha, \alpha \in \mathcal{J}^{N,K}\}$ shows as Table 1.

*4.1.2. Moment Estimation.* Furthermore, we use the SG method to find the coefficients of random function (Equation (19)), and Table 2 summarizes our result.

Table 3 shows the exact mean and the approximate mean of random function (Equation (19)), the exact variance and the approximate variance, and the error between them, respectively.

Table 1: Orthogonal basis for bivariate Gaussian random variables.

| |
|---|
| $\Phi_0 = 1$ |
| $\Phi_1 = \xi_2 - 1$ |
| $\Phi_2 = 1.25\xi_1 - 0.75\xi_2 - 0.5$ |
| $\Phi_3 = 0.8575\xi_1\xi_2 - 0.858\xi_2 - 0.8574\xi_1 + 0.3428$ |
| $\Phi_4 = 1.0308\xi_1^2 - 0.9078\xi_1\xi_2 - 1.1538\xi_1 + 0.9077\xi_2 - 0.3632$ |
| $\Phi_5 = 1.10485\xi_2^2 + 0.3959\xi_1^2 + 0.52944\xi_1 - 0.88775\xi_2$ $- 1.3213\xi_1\xi_2 - 0.52845$ |

*4.1.3. Density Estimation.* Based on Algorithm 1 and Tables 1 and 2, we can obtain the truncated expansion for the random function and calculated its probability density function (PDF). In order to sampling, we taken each dimension has the same sample size, $\mathcal{S} = S_i$, $(i = 1, 2, \ldots, K)$.

$$f(\xi_1, \xi_2) = \sum_{m=0}^{M} \widehat{f}_m \Phi_m(\xi_1, \xi_2), \tag{20}$$

$$f(\widetilde{\xi}_1, \widetilde{\xi}_2) = \sum_{m=0}^{M} \widehat{f}_m \Phi_m(\widetilde{\xi}_1, \widetilde{\xi}_2). \tag{21}$$

$(\tilde{\xi}_1, \tilde{\xi}_2)$ are sample points according to $\rho(\xi_1, \xi_2)$. Here, approximation uses $\mathcal{S} = 1000$ sample points. We used square Euclidean distance to describe the error of gPC-based density estimation.

$$\text{Error}_{\text{gPC-based}} = \frac{1}{\sqrt{2}} \sum \left(\sqrt{p_f} - \sqrt{p_{f_N}}\right)^2. \tag{22}$$

Figure 1(c) shows the error of gPC-based are larger (red dotted line) when the number of basis function $M \leq 4$, and the error has the spectral accuracy when $M \geq 5$ (blue dotted line).

Table 2: The coefficients of $\widehat{f}_\alpha$ corresponding to orthogonal basis.

| | | | | | |
|---|---|---|---|---|---|
| $\widehat{f}_0 = 0.4$ | $\widehat{f}_1 = -0.4$ | $\widehat{f}_2 = 0.8$ | $\widehat{f}_3 = -0.1372$ | $\widehat{f}_4 = 0.9698$ | $\widehat{f}_5 = -0.0022$ |

Table 3: The random function $f(\xi_1, \xi_2)$: the exact mean, the approximate mean and error between them (the first row); the exact variance, the approximate variance and error between them (the second row).

| | | |
|---|---|---|
| $\mathbb{E}[f(\xi_1, \xi_2)]$ | $\mathbb{E}[f_M(\xi_1, \xi_2)]$ | $\mathbb{E}[f(\xi_1, \xi_2) - f_M(\xi_1, \xi_2)]$ |
| 0.4 | 0.3999959359 | $4.0641E-6$ |
| $\mathrm{Var}[f(\xi_1, \xi_2)]$ | $\mathrm{Var}[f_M(\xi_1, \xi_2)]$ | $\mathrm{Var}[f(\xi_1, \xi_2)] - \mathrm{Var}[f_M(\xi_1, \xi_2)]$ |
| 1.76 | 1.75921322 | $7.8678E-4$ |

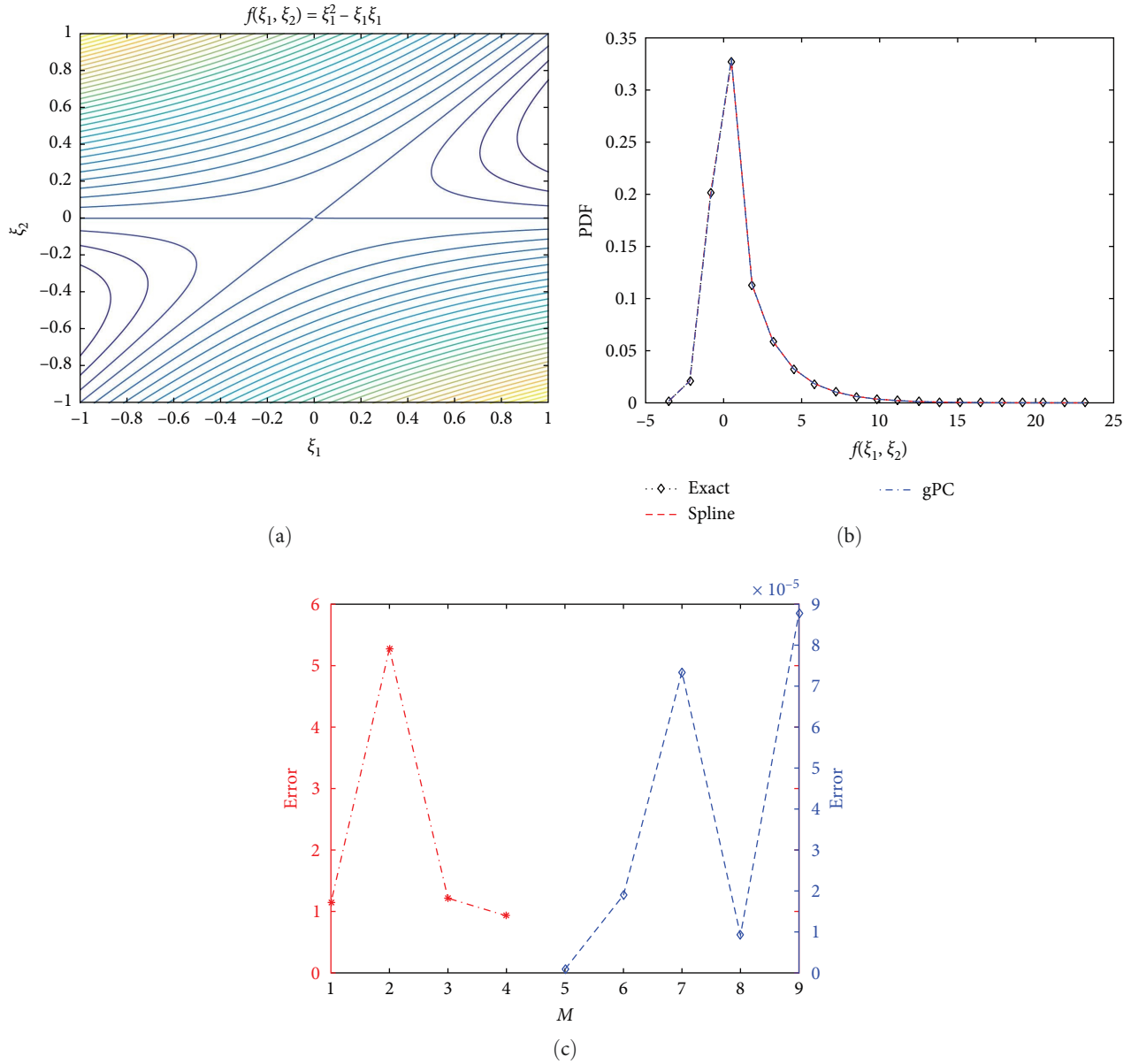


Figure 1: (a) Contours of the random function $f(\xi_1, \xi_2)$. (b) The PDF of $f(\xi_1, \xi_2)$ (black diamond dotted line), the red line and blue line represent its approximation by multidimensional spline-based and gPC-based Algorithm 1, respectively. (c) The error of PDF by gPC-based approximation with the number of basis function.

Table 4: The random function $f(\xi_1, \xi_2)$: the exact mean, the approximate mean by Monte-Carlo simulation and error between them (the first row); the exact variance, the approximate variance by Monte-Carlo simulation and error between them (the second row).

| $\mathfrak{T} = 10^3$ | $\mathfrak{T} = 10^4$ | $\mathfrak{T} = 10^5$ | $\mathfrak{T} = 10^6$ | $\mathfrak{T} = 10^7$ | $\mathfrak{T} = 10^8$ |
|---|---|---|---|---|---|
| 0.0241 | 0.0056 | 0.005 | $2.0633E-4$ | $4.4070E-4$ | $3.4844E-5$ |
| 0.0162 | 0.0314 | 0.0083 | 0.0019 | 0.0021 | $5.0490E-4$ |

$\mathfrak{T}$ represents the sample size of Monte-Carlo simulation.

Table 5: The random function $f(\xi_1, \xi_2)$: the exact PDF, the approximate PDF by Monte-Carlo simulation and error between them.

| $\mathfrak{T} = 100$ | $\mathfrak{T} = 1000$ | $\mathfrak{T} = 10^4$ | $\mathfrak{T} = 10^5$ | $\mathfrak{T} = 10^6$ | $\mathfrak{T} = 10^7$ | $\mathfrak{T} = 10^8$ |
|---|---|---|---|---|---|---|
| 1.4450 | 1.1056 | 0.8846 | 0.8006 | 0.6930 | 0.6770 | 0.5364 |

$\mathfrak{T}$ represents the sample size of Monte-Carlo simulation.

Table 6: The random function $u(x, t, \xi_1, \xi_2)$: the approximate mean (the first row) and the approximate variance (the second row) at different times ($t = 0, 5, 10, 20$) when $x = 0$.

| $t$ | 0 | 5 | 10 | 20 |
|---|---|---|---|---|
| $\mathbb{E}[u]$ | 0.4516 | 0.0617 | 0.0199 | 0.0087 |
| $\mathrm{Var}[u]$ | 0.2258 | 0.0068 | 0.0012 | $2.6823E-4$ |

*4.1.4. Efficiency.* In this section, we focus on moment estimation and density estimation for random function $f(\xi_1, \xi_2)$ in contrast to Monte-Carlo simulation with different sample sizes.

Table 4 shows the mean and variance of $f(\xi_1, \xi_2)$ by Monte-Carlo simulation; the error of mean and variance gets smaller and smaller when the sample size of simulation multiplies. In contrast to Table 3, it can be seen that high-order methods are spectral accuracy when the degrees of basis function are two orders ($N = 2$). The error of mean and variance by Monte-Carlo simulation can be spectral accuracy when the sample size is enormous amount ($\mathfrak{T} = 10^8$).

Table 5 shows the PDF error of $f(\xi_1, \xi_2)$ by Monte-Carlo simulation. In contrast to Figure 1, the proposed method can achieve high precision with only six expansion terms, and Monte-Carlo simulation requires a huge amount of computation to achieve close precision. Although the accuracy of Monte-Carlo simulation is limited and the calculation cost is high, this method is easy to implement and is very simple and useful. Then it can be seen that high-order methods are superior to the Monte-Carlo simulation, as it gives sufficiently accurate results [29, 30].

*4.2. Application.* In this section, we used the gPC-based density estimation to the stochastic 1D wave equation and Stochastic 2D Schnakenberg model. We assume that the unknown function has periodic boundary conditions in the $x-$ or $y-$ direction, and we will use the Fourier spectral method to approximate the unknown function $u$ in the $x-$ or $y-$ direction [31–33]. The $(\xi_1, \xi_2)$ are bivariate Gaussian distribution, same as Equation (19).

*4.2.1. Stochastic 1D Wave Equation.* The stochastic 1D wave equation.

$$\begin{aligned} &\frac{\partial^2 u}{\partial t^2} = \xi_1^2 \frac{\partial^2 u}{\partial x^2}, \ x \in [-40, 40], \\ &u_0(x) = \xi_2 \mathrm{sech}(x), \end{aligned} \tag{23}$$

where $\vec{x} = x$.

Table 6 shows the mean and variance of $u(x, t, \xi_1, \xi_2)$ at different time $(t = 0, 5, 10, 20)$ when $x = 0$. With the passage of time, the mean amplitude of the wave gradually decreases, and the variance gradually decreases and tends to zero, while Figure 2 (top and middle) also demonstrates this phenomenon. When $t = 0, x = 0$, the $\mathbb{E}[u(0, 0, \xi_1, \xi_2)]$ evaluated at point 0.5, so, the value of PDF for $u(0, 0, \xi_1, \xi_2)$ are huge at location $u$ nearby point 0.5.

$$\begin{aligned} &\mathbb{P}\{u(0, 0, \xi_1, \xi_2) \geq 0.5\} \\ &= 1 - \mathbb{P}\{u(0, 0, \xi_1, \xi_2) < 0.5\} \overset{\text{almost}}{=} 1. \end{aligned} \tag{24}$$

As the wave energy dissipates, the value of PDF for $u(0, 5, \xi_1, \xi_2)$ and $u(0, 10, \xi_1, \xi_2)$ gradually close to the location of $u$ nearby zero.

$$\mathbb{P}\{-0.2 \leq u(0, 0, \xi_1, \xi_2) \leq 0.2\} \overset{\text{almost}}{=} 1. \tag{25}$$

Until the wave energy almost runs out, the value of PDF for $u(0, 20, \xi_1, \xi_2)$ evaluated at location of u nearby zero and the interval length of $u(0, 20, \xi_1, \xi_2)$ is small than before. At the location of $u(0, 0, \xi_1, \xi_2) = 0$, the value of PDF for $u(0, 0, \xi_1, \xi_2)$ almost equal to 1.

$$\mathbb{P}\{0 - \delta \leq u(0, 0, \xi_1, \xi_2) \leq 0 + \delta\} \overset{\text{almost}}{=} 1, \tag{26}$$

where $(0 - \delta, 0 + \delta)$ is a small neighborhood with centered on 0 point.

*4.2.2. Stochastic 2D Schnakenberg Model.* The Stochastic 2D Schnakenberg model and Schnakenberg model belong to the reaction-diffusion system.

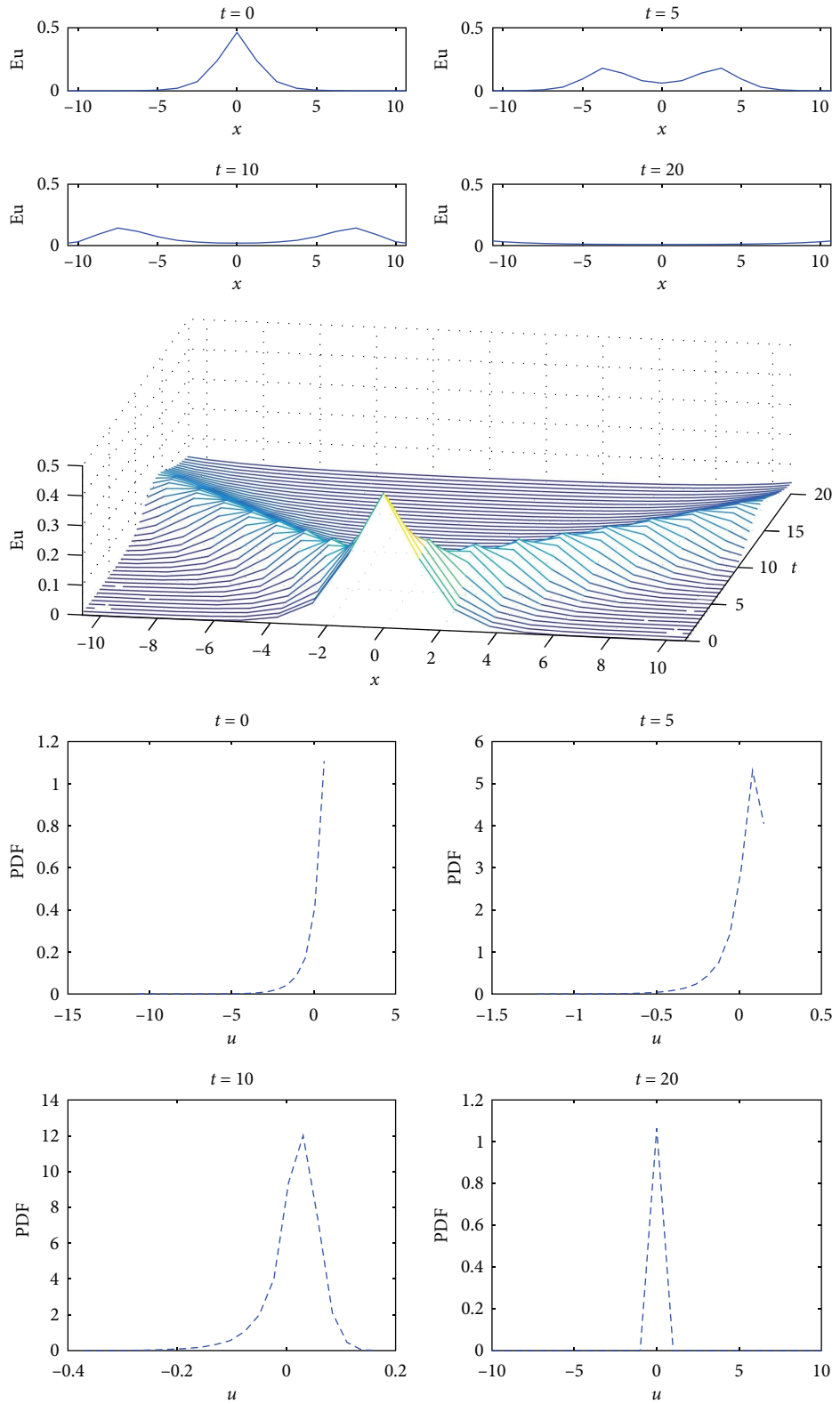


FIGURE 2: The mean amplitude of Equation (23) solution at different times ($t = 0, 5, 10, 20$ (top)). The trend fluctuations of mean amplitude for Equation (23) solution at every time (middle). The PDF of Equation (23) solution at different times ($t = 0, 5, 10, 20$ (bottom)).

Table 7: The random function $u(x, y, t, \xi_1, \xi_2)$: the approximate mean (the first row) and the approximate variance (the second row) at different times ($t = 0$, 0.05, 0.1, 0.15) when $(x = 0, y = 0)$.

| $t$ | 0 | 0.05 | 0.1 | 0.15 |
|---|---|---|---|---|
| $\mathbb{E}[u]$ | 0 | 0.7934 | 0.7429 | 0.7436 |
| Var$[u]$ | 0 | $4.8203E-5$ | $4.111E-5$ | $4.2182E-5$ |

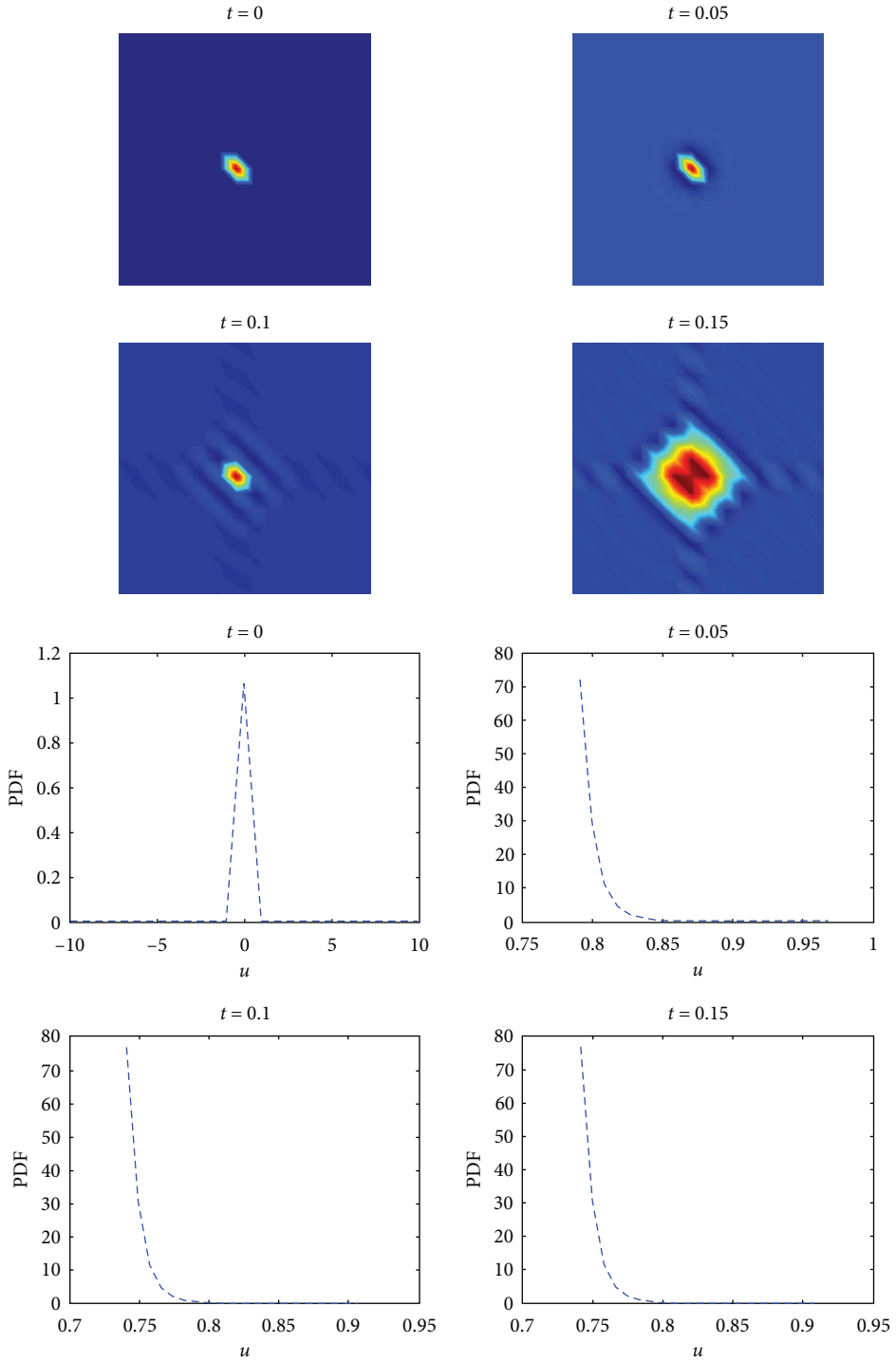


Figure 3: The pattern transformation and PDF function for the Schnakenberg model at different times ($t = 0$, 0.05, 0.1, 0.15).

$$\begin{aligned}\frac{\partial u}{\partial t} &= \left(\frac{\partial^2}{\partial x^2}+\frac{\partial^2}{\partial y^2}\right)u+\gamma(\xi_1-u+u^2v),\\ \frac{\partial v}{\partial t} &= d\left(\frac{\partial^2}{\partial x^2}+\frac{\partial^2}{\partial y^2}\right)v+\gamma(\xi_2-u^2v),\end{aligned} \tag{27}$$

where $\vec{x}=(x,y)\in\{[-\pi,\pi]\times[-\pi,\pi]\}$, $\gamma=100, d=26$.

In stochastic 2D Schnakenberg model, $u(x,y,t,\xi_1,\xi_2)$ and $v(x,y,t,\xi_1,\xi_2)$ can be described as the concentration of some material. Table 7 shows the mean and variance of $u(x,y,t,\xi_1,\xi_2)$ at different time $(t=0,0.05,0.1,0.15)$ when $x=y=0$. From Table 5, we know, as the beginning, the mean and variance of $u(0,0,0,\xi_1,\xi_2)$ is zero, and the mean and variance of $u(0,0,0.05,\xi_1,\xi_2)$ is increase when time increase. when $t=0.05$, the mean and variance of $u(0,0,0.05,\xi_1,\xi_2)$ almost same as $u(0,0,0.1,\xi_1,\xi_2)$ and $u(0,0,0.15,\xi_1,\xi_2)$, just a small change when time increase.

When $t=0,x=y=0$, the $\mathbb{E}[u(0,0,0,\xi_1,\xi_2)]$ equal zero, so, the value of PDF for $u(0,0,0,\xi_1,\xi_2)$ evaluated at location of $u$ nearby zero and the interval length of $u(0,0,0,\xi_1,\xi_2)$ is small.

$$\mathbb{P}\{0-\delta\le u(0,0,0,\xi_1,\xi_2)\le 0+\delta\}\overset{\text{almost}}{=}1, \tag{28}$$

where $(0-\delta,0+\delta)$ is a small neighborhood with centered on 0 point.

As the reaction goes on, the value of PDF for $u(0,0,0.05,\xi_1,\xi_2)$, and $u(0,0,0.15,\xi_1,\xi_2)$ almost same each other with little change.

$$\begin{aligned}&\mathbb{P}\{u(0,0,0,\xi_1,\xi_2)\le 0.85\}\\ &=1-\mathbb{P}\{u(0,0,0,\xi_1,\xi_2)>0.85\}\overset{\text{almost}}{=}1.\end{aligned} \tag{29}$$

The pattern of Figure 3 demonstrates the mean concentration of $u(x,y,t,\xi_1,\xi_2)$ transformation phenomenon at different times (0, 0.05, 0.1, 0.15).

## 5. Concluding Remarks

We have proposed a newly high-order spectral numerical method for the density estimation of bivariate Gaussian random variables, based on gPC expansion. The new method can be of spectral accuracy in space and as well as in random space, at least for some smooth problems. This efficient and accurate numerical method was applied to study moment estimation and density estimation for stochastic 1D wave equation and stochastic 2D Schnakenberg model, respectively. In the future, we plan to construct the analytic formula of the cumulative distribution function for the unknown solution of stochastic partial/ordinary differential equation driven by multivariate Gaussian random variables.

## Data Availability

No data were used to support this study.

## Conflicts of Interest

The author declares that they have no conflicts of interest.

## References


[1] O. P. Le Maître, L. Mathelin, O. M. Knio, and M. Yousuff Hussaini, "Asynchronous time integration for polynomial chaos expansion of uncertain periodic dynamics," *Discrete and Continuous Dynamical Systems*, vol. 28, no. 1, pp. 199–226, 2010.

[2] H. N. Najm, "Uncertainty quantification and polynomial chaos techniques in computational fluid dynamics," *Annual Review of Fluid Mechanics*, vol. 41, pp. 35–52, 2009.

[3] A. Ditkowski, G. Fibich, and A. Sagiv, "Density estimation in uncertainty propagation problems using a surrogate model," *SIAM/ASA Journal on Uncertainty Quantification*, vol. 8, no. 1, pp. 261–300, 2020.

[4] B. Sudret and A. Der Kiureghian, "Stochastic finite element methods and reliability: a state-of-the-art report," Department of Civil and Environmental Engineering, University of California, Berkeley, 2000.

[5] I. Colombo, F. Nobile, G. Porta, A. Scotti, and L. Tamellini, "Uncertainty quantification of geochemical and mechanical compaction in layered sedimentary basins," *Computer Methods in Applied Mechanics and Engineering*, vol. 328, pp. 122–146, 2018.

[6] N. N. Madras, *Lectures on Monte Carlo Methods*, American Mathematical Soc., 2002.

[7] M. Kamiński, "Uncertainty analysis in solid mechanics with uniform and triangular distributions using stochastic perturbation-based Finite Element Method," *Finite Elements in Analysis and Design*, vol. 200, Article ID 103648, 2022.

[8] H. Xie, "An efficient and spectral accurate numerical method for computing SDE driven by multivariate Gaussian variables," *AIP Advances*, vol. 12, no. 7, Article ID 075306, 2022.

[9] S. Rahman, "Wiener–Hermite polynomial expansion for multivariate Gaussian probability measures," *Journal of Mathematical Analysis and Applications*, vol. 454, no. 1, pp. 303–334, 2017.

[10] S. Rahman, "A polynomial chaos expansion in dependent random variables," *Journal of Mathematical Analysis and Applications*, vol. 464, no. 1, pp. 749–775, 2018.

[11] J. D. Jakeman, F. Franzelin, A. Narayan, M. Eldred, and D. Plfüger, "Polynomial chaos expansions for dependent random variables," *Computer Methods in Applied Mechanics and Engineering*, vol. 351, pp. 643–666, 2019.

[12] M. Chevreuil, R. Lebrun, A. Nouy, and P. Rai, "A least-squares method for sparse low rank approximation of multivariate functions," *SIAM/ASA Journal on Uncertainty Quantification*, vol. 3, no. 1, pp. 897–921, 2015.

[13] A. Doostan and H. Owhadi, "A non-adapted sparse approximation of PDEs with stochastic inputs," *Journal of Computational Physics*, vol. 230, no. 8, pp. 3015–3034, 2011.

[14] J. D. Jakeman, M. S. Eldred, and K. Sargsyan, "Enhancing $\mathfrak{l}_1$-minimization estimates of polynomial chaos expansions using basis selection," *Journal of Computational Physics*, vol. 289, pp. 18–34, 2015.

[15] T. Tang and T. Zhou, "On discrete least-squares projection in unbounded domain with random evaluations and its application to parametric uncertainty quantification," *SIAM Journal on Scientific Computing*, vol. 36, no. 5, pp. A2272–A2295, 2014.

[16] J. A. S. Witteveen and H. Bijl, "Modeling arbitrary uncertainties using Gram-Schmidt polynomial chaos," in *44th AIAA Aerospace Sciences Meeting and Exhibit*, pp. 1–17, ARC, 2006.
[17] L. Yan, L. Guo, and D. Xiu, "Stochastic collocation algorithms using ℓ1-minimization," *International Journal for Uncertainty Quantification*, vol. 2, no. 3, pp. 279–293, 2012.
[18] M. Navarro, J. Witteveen, and J. Blom, "Polynomial chaos expansion for general multivariate distributions with correlated variables," 2014.
[19] E. Savinov and V. Shamraeva, "On a Rosenblatt-type transformation of multivariate copulas," *Econometrics and Statistics*, vol. 25, pp. 39–48, 2023.
[20] M. Zhang, A. Zhang, and Y. Zhou, "Construction of uniform designs on arbitrary domains by inverse rosenblatt transformation," in *Contemporary Experimental Design, Multivariate Analysis and Data Mining*, pp. 111–126, Springer, 2020.
[21] P. K. Sen, "Introduction to nonparametric estimation by Alexandre B. Tsybakov," *International Statistical Review*, vol. 79, no. 2, pp. 291-292, 2011.
[22] L. Wasserman, *All of Statistics: A Concise Course in Statistical Inference*, Springer, New York, 2004.
[23] É. Savin and B. Faverjon, "Computation of higher-order moments of generalized polynomial chaos expansions," *International Journal for Numerical Methods in Engineering*, vol. 111, no. 12, pp. 1192–1200, 2017.
[24] W. Luo, "Wiener chaos expansion and numerical solutions of stochastic partial differential equations," California Institute of Technology, Ph.D. dissertation, 2006.
[25] L. N. Trefethen, *Approximation Theory and Approximation Practice, Extended Edition*, SIAM, 2019.
[26] H. Wang and S. Xiang, "On the convergence rates of Legendre approximation," *Mathematics of Computation*, vol. 81, pp. 861–877, 2012.
[27] D. Xiu, *Numerical Methods for Stochastic Computations: A Spectral Method Approach*, Princeton University Press, 2010.
[28] J. S. Hesthaven, S. Gottlieb, and D. Gottlieb, *Spectral Methods for Time-dependent Problems*, Cambridge University Press, 2007.
[29] S. Oladyshkin and W. Nowak, "Incomplete statistical information limits the utility of high-order polynomial chaos expansions," *Reliability Engineering & System Safety*, vol. 169, pp. 137–148, 2018.
[30] Q. Zhang and L. Xu, "Evaluation of moments of performance functions based on polynomial chaos expansions," *International Journal of Mechanics and Materials in Design*, vol. 18, pp. 395–405, 2022.
[31] R. Cheng, L. Wu, C. Pang, and H. Wang, "A Fourier collocation method for Schrödinger–Poisson system with perfectly matched layer," *Communications in Mathematical Sciences*, vol. 20, no. 2, pp. 523–542, 2022.
[32] J. Shen, T. Tang, and L.-L. Wang, *Spectral Methods: Algorithms, Analysis and Applications*, Springer Science & Business Media, 2011.
[33] H. Wang, "A time-splitting spectral method for coupled Gross–Pitaevskii equations with applications to rotating Bose–Einstein condensates," *Journal of Computational and Applied Mathematics*, vol. 205, no. 1, pp. 88–104, 2007.